JCI The Journal of Clinical Investigation

CD19 CAR–T cells of defined CD4$^+$:CD8$^+$ composition in adult B cell ALL patients

Cameron J. Turtle, Laïla-Aïcha Hanafi, Carolina Berger, Theodore A. Gooley, Sindhu Cherian, Michael Hudecek, Daniel Sommermeyer, Katherine Melville, Barbara Pender, Tanya M. Budiarto, Emily Robinson, Natalia N. Steevens, Colette Chaney, Lorinda Soma, Xueyan Chen, Cecilia Yeung, Brent Wood, Daniel Li, Jianhong Cao, Shelly Heimfeld, Michael C. Jensen, Stanley R. Riddell, David G. Maloney

J Clin Invest. 2016. https://doi.org/10.1172/JCI85309.

Clinical Research and Public Health | Oncology

BACKGROUND. T cells that have been modified to express a CD19-specific chimeric antigen receptor (CAR) have antitumor activity in B cell malignancies; however, identification of the factors that determine toxicity and efficacy of these T cells has been challenging in prior studies in which phenotypically heterogeneous CAR–T cell products were prepared from unselected T cells.

METHODS. We conducted a clinical trial to evaluate CD19 CAR–T cells that were manufactured from defined CD4$^+$ and CD8$^+$ T cell subsets and administered in a defined CD4$^+$:CD8$^+$ composition to adults with B cell acute lymphoblastic leukemia after lymphodepletion chemotherapy.

RESULTS. The defined composition product was remarkably potent, as 27 of 29 patients (93%) achieved BM remission, as determined by flow cytometry. We established that high CAR–T cell doses and tumor burden increase the risks of severe cytokine release syndrome and neurotoxicity. Moreover, we identified serum biomarkers that allow testing of early intervention strategies in patients at the highest risk of toxicity. Risk-stratified CAR–T cell dosing based on BM disease burden decreased toxicity. CD8$^+$ T cell–mediated anti-CAR transgene product immune responses developed after CAR–T cell infusion in some patients, limited CAR–T cell persistence, and increased relapse risk. Addition of fludarabine to the lymphodepletion regimen improved CAR–T cell persistence and disease-free survival.

CONCLUSION. Immunotherapy with a CAR–T cell product of defined composition enabled identification of factors […]

Find the latest version:

https://jci.me/85309/pdf

CD19 CAR–T cells of defined CD4+:CD8+ composition in adult B cell ALL patients

Cameron J. Turtle,[1,2] Laïla-Aïcha Hanafi,[1] Carolina Berger,[1,2] Theodore A. Gooley,[1] Sindhu Cherian,[3] Michael Hudecek,[1] Daniel Sommermeyer,[1] Katherine Melville,[1] Barbara Pender,[1] Tanya M. Budiarto,[1] Emily Robinson,[1] Natalia N. Steevens,[1] Colette Chaney,[1] Lorinda Soma,[3] Xueyan Chen,[3] Cecilia Yeung,[3,4] Brent Wood,[3,4] Daniel Li,[5] Jianhong Cao,[1] Shelly Heimfeld,[1] Michael C. Jensen,[1,6] Stanley R. Riddell,[1,2,7] and David G. Maloney[1,2]

[1]Clinical Research Division, Fred Hutchinson Cancer Research Center (FHCRC), Seattle, Washington, USA. [2]Department of Medicine, [3]Department of Laboratory Medicine, and [4]Department of Pathology, University of Washington, Seattle, Washington, USA. [5]Juno Therapeutics, Seattle, Washington, USA. [6]Seattle Children's Research Institute, Seattle, Washington, USA. [7]Institute for Advanced Study, Technical University of Munich, Munich, Germany.

BACKGROUND. T cells that have been modified to express a CD19-specific chimeric antigen receptor (CAR) have antitumor activity in B cell malignancies; however, identification of the factors that determine toxicity and efficacy of these T cells has been challenging in prior studies in which phenotypically heterogeneous CAR–T cell products were prepared from unselected T cells.

METHODS. We conducted a clinical trial to evaluate CD19 CAR–T cells that were manufactured from defined CD4+ and CD8+ T cell subsets and administered in a defined CD4+:CD8+ composition to adults with B cell acute lymphoblastic leukemia after lymphodepletion chemotherapy.

RESULTS. The defined composition product was remarkably potent, as 27 of 29 patients (93%) achieved BM remission, as determined by flow cytometry. We established that high CAR–T cell doses and tumor burden increase the risks of severe cytokine release syndrome and neurotoxicity. Moreover, we identified serum biomarkers that allow testing of early intervention strategies in patients at the highest risk of toxicity. Risk-stratified CAR–T cell dosing based on BM disease burden decreased toxicity. CD8+ T cell–mediated anti-CAR transgene product immune responses developed after CAR–T cell infusion in some patients, limited CAR–T cell persistence, and increased relapse risk. Addition of fludarabine to the lymphodepletion regimen improved CAR–T cell persistence and disease-free survival.

CONCLUSION. Immunotherapy with a CAR–T cell product of defined composition enabled identification of factors that correlated with CAR–T cell expansion, persistence, and toxicity and facilitated design of lymphodepletion and CAR–T cell dosing strategies that mitigated toxicity and improved disease-free survival.

TRIAL REGISTRATION. ClinicalTrials.gov NCT01865617.

FUNDING. R01-CA136551; Life Science Development Fund; Juno Therapeutics; Bezos Family Foundation.

Introduction

The administration of lymphodepleting chemotherapy followed by adoptive transfer of autologous T cells that are genetically modified to express a chimeric antigen receptor (CAR) specific for CD19 (CD19 CAR–T cells) has produced a high rate of complete remission (CR) in adult and pediatric patients with relapsed and refractory B cell acute lymphoblastic leukemia (B-ALL) in small phase I clinical trials (1–4). Encouraging results have also been seen in clinical trials of CD19 CAR–T cell therapy in non-Hodgkin's lymphoma (NHL) and chronic lymphocytic leukemia (CLL) (5–9). Emerging data from these studies suggest that robust proliferation of transferred CAR–T cells in the recipient correlates with clinical response and that prolonged in vivo persistence of functional CAR–T cells may be necessary to prevent disease relapse. The administration of CD19 CAR–T cells and their subsequent expansion can be associated with cytokine release syndrome (CRS), characterized by hyperpyrexia, hypotension, capillary leak, neurotoxicity, and death in severe cases (3, 4, 7, 9, 10). The factors that determine CAR–T cell expansion and persistence in vivo, the durability of antitumor responses, and toxicities have been challenging to define in initial studies in part because of the wide vari-

Authorship note: S.R. Riddell and D.G. Maloney contributed equally to this work.
Conflict of interest: C.J. Turtle receives research funding from Juno Therapeutics. D.G. Maloney receives research funding from Juno Therapeutics. S.R Riddell and M.C. Jensen receive research funding from and are cofounders of Juno Therapeutics. D. Li is an employee of and has equity in Juno Therapeutics. C. Yeung receives unrelated research funding from Gilead Sciences. C. Berger receives research funding from Juno Therapeutics. S.R. Riddell, M. Hudecek, and M.C. Jensen have a related patent (US-2015-0306141). S.R. Riddell, C. Berger, and M.C. Jensen have a related patent (US-2014-0356398). M.C. Jensen has a related patent (US8802374 B2).
Role of funding source: Personnel from Juno Therapeutics reviewed the draft manuscript and assisted with statistical analyses, but were not involved in recruitment or clinical care of participants, performance of response assessments, or conduct of laboratory assays. Personnel from the other funding sources did not contribute to the design, conduct, or analysis of the study.
Submitted: November 5, 2015; **Accepted:** March 8, 2016.
Reference information: *J Clin Invest*. doi:10.1172/JCI85309.

ation in CAR–T cell doses administered to patients, differences in the phenotypic composition of T cells isolated from patients for genetic modification and in the infused products, and differences in chemotherapy regimens administered to patients to provide lymphodepletion before CAR–T cells are infused (11).

Prior work has demonstrated that human $CD4^+$ and $CD8^+$ T cells comprise functionally and transcriptionally distinct subsets that differ in their capacities to proliferate and persist in vivo after in vitro expansion and adoptive transfer (12–16). Using a preclinical model, we demonstrated that human CD19 CAR–T cells that were manufactured from purified $CD8^+$ or $CD4^+$ central memory T cells (T_{CM} cells) or naive T cells (T_N cells) were more potent in elimination of $CD19^+$ tumors from immunodeficient mice compared with CD19 CAR–T cells that were manufactured from effector memory T cells (T_{EM} cells) (17). Synergistic enhancement in potency could be achieved by infusion of a defined ratio of CD19 CAR–T cells derived from $CD8^+$ T_{CM} cells and $CD4^+$ T cells. These results suggested that selecting defined subsets of T cells from patients with B-ALL prior to transduction and formulating therapeutic CAR–T cell products of uniform composition might provide reproducible potency in clinical therapy and facilitate determining potential correlations between cell dose and efficacy or toxicity. Thus, we initiated a phase I/II clinical trial in patients with refractory B-ALL in which $CD8^+$ and $CD4^+$ T cell subsets were separately modified to express a CD19-targeted CAR incorporating 4-1BB and CD3ζ signaling domains, formulated in a defined ratio of $CD4^+$:$CD8^+$ CAR–T cells, and administered in a dose-escalation/deescalation format after lymphodepletion with a cyclophosphamide-based (Cy-based) regimen, alone or with fludarabine (Flu).

The eligibility criteria for this study did not exclude any patient based on the absolute lymphocyte count or on a predetermined measurement of the ability of the patient's T cells to expand after activation with anti-CD3/CD28 beads. Our data show that a therapeutic CAR–T cell product could be manufactured from all patients that enrolled in the study and that formulation of CAR–T cells in a defined composition was feasible in a majority of these heavily pretreated patients. We observed reproducible in vivo proliferation of CAR–T cells and antitumor activity, and low doses (2×10^5/kg) of the defined-composition CAR–T cell product were remarkably potent for inducing CR without a high rate of toxicity in patients with a high tumor burden. We demonstrate that a T cell–mediated immune response specific for epitopes encoded by the CAR transgene can develop in some patients who receive Cy lymphodepletion and limit the persistence of transferred CAR–T cells. The persistence of CAR–T cells, duration of remission, and disease-free survival (DFS) were improved by the addition of Flu to the lymphodepleting chemotherapy regimen.

Results

Patient characteristics. Thirty-two consecutive patients with relapsed or refractory $CD19^+$ B-ALL and a median age of 40 years (range 20–73) that enrolled in the study had CD19 CAR–T cells manufactured (Figure 1A). Two patients developed complications related to prior treatment during CAR–T cell manufacturing that excluded them from receiving lymphodepletion chemotherapy and CAR–T cells. One of these patients died due to progressive B-ALL, and the other is alive, at this writing, with persistent B-ALL. The 30 patients who proceeded to lymphodepletion chemotherapy and CD19 CAR–T cell infusion had previously received a median of 3 prior intensive chemotherapy regimens (range 1–11), and 11 patients had relapsed at a median of 7 months (range 1–28) after prior allogeneic hematopoietic cell transplantation (HCT) (Table 1). Before lymphodepletion and CAR–T cell therapy, all patients had detectable disease in BM, extramedullary sites, or cerebrospinal fluid (CSF). Twenty-nine of 30 patients had detectable leukemic blasts in the BM (median 21.0%, range 0.014%–97.0%, $n = 29$), and 7 patients had extramedullary disease, including 5 with bulky extramedullary disease. Leukemia was detected by flow cytometry in the CSF from 2 patients, one of whom had no other identified site of disease. The other 28 patients were negative for leukemic blasts in the CSF at evaluation before CAR–T cell infusion.

Prior to leukapheresis, we evaluated the absolute counts and proportions of T_N, T_{CM}, and $T_{EM/EMRA}$ (where T_{EMRA} indicates $CD45RA^+$ effector memory) cells within the $CD4^+$ and $CD8^+$ T cell subsets in the blood of each B-ALL patient (Figure 1, B–E). B-ALL patients had lower numbers of $CD4^+$ and $CD8^+$ T cells compared with healthy individuals (Figure 1C), and the $CD4^+$:$CD8^+$ T cell ratio was highly variable within the patient population (median 1.19; range 0.27–8.89). Importantly, we found marked heterogeneity in the percentages of $T_{EM/EMRA}$ cells within the $CD4^+$ and $CD8^+$ T cell subsets in B-ALL patients (Figure 1, D and E; $CD4^+$ $T_{EM/EMRA}$, range 7.8%–57.5%; $CD8^+$ $T_{EM/EMRA}$, range 8.5%–87.4%). These data suggest that, particularly in B-ALL patients who have high fractions of $T_{EM/EMRA}$ or a disparate ratio of $CD4^+$:$CD8^+$ T cells in blood, the ability to manufacture a CD19 CAR–T cell product of consistent potency may be enhanced by selection of defined T cell subsets from the leukapheresis product for CAR gene transfer and formulation of the CAR–T cell product in a defined $CD4^+$:$CD8^+$ CAR–T cell ratio.

CD19 CAR–T cell manufacturing. There were no serious adverse events in the 32 patients who underwent leukapheresis. Highly enriched $CD4^+$ T cells were isolated for CAR–T cell manufacturing from all patients ($CD3^+CD4^+$ T cell purity 97.2%; range 48.5%–99.6%; $n = 32$). Our preclinical studies had suggested that infusion of $CD8^+$ T_{CM} CAR–T cells combined with $CD4^+$ CAR–T cells might provide optimal antitumor efficacy and that an absolute $CD8^+$ T_{CM} cell count of 20/μl or more on a screening assay was necessary for efficient selection of $CD8^+$ T_{CM} cells using a sequential 2-step enrichment that involved depletion of $CD4^+CD14^+CD45RA^+$ cells followed by selection of $CD62L^+$ cells (ref. 18 and Supplemental Figure 1, A and B; supplemental material available online with this article; doi:10.1172/JCI85309DS1). Enrichment of $CD8^+$ T_{CM} cells using this approach was successful in 18 of 19 patients. For the patients undergoing $CD8^+$ T_{CM} selection, the frequency of $CD3^+CD8^+$ T cells with a $CD45RA^-$ $CD62L^+$ phenotype increased from 13.2% (range 1.12%–41.8%) in the leukapheresis product to 72.2% (range 24.5%–90.2%) after the 2-step enrichment. $CD3^+CD8^+$ T cells made up 17.4% (range 0.86%–66.9%) of the $CD4^-CD14^-CD45RA^-CD62L^+$ product, with the remainder being $CD13^+CD15^+CD16^+$ myeloid cells and $CD13^+CD123^+CD16^-$ basophils (Supplemental Figure 1, B and C). Fourteen patients, including one who had an unsuccessful $CD8^+$ T_{CM} selection, had profound lymphopenia ($CD4^+$, median 150

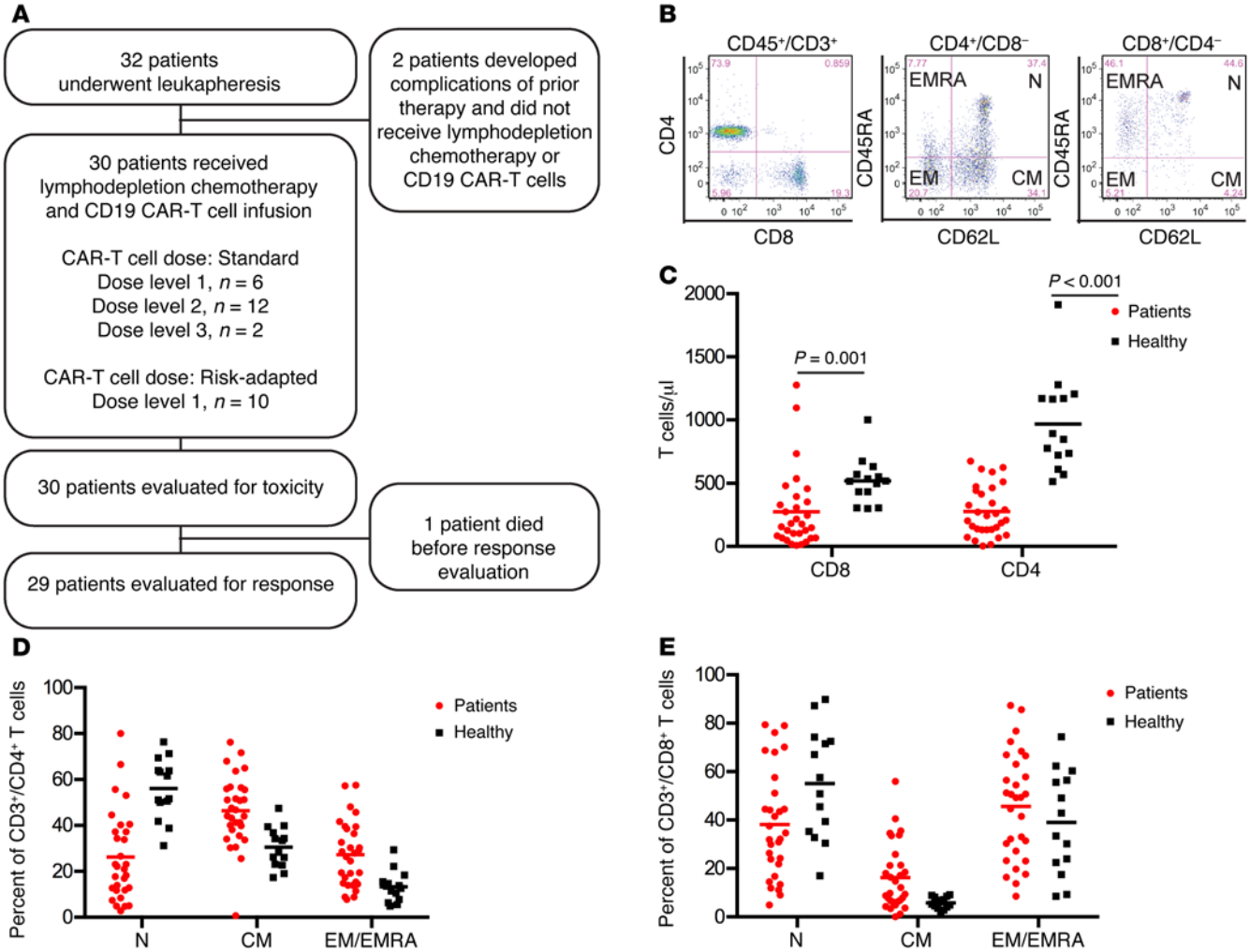

Figure 1. Heterogeneity in distribution of T_N, T_{CM}, and $T_{EM/EMRA}$ cells within CD4⁺ and CD8⁺ T cell subsets in normal donors and patients with B-ALL. (**A**) Study participant flow chart. (**B**) Representative flow cytometry plots showing the immunophenotype of T cell subsets in blood from a B-ALL patient are shown. T_N (CD45RA⁺CD62L⁺), T_{CM} (CD45RA⁻CD62L⁺), and $T_{EM/EMRA}$ (CD62L⁻) cells can be identified in the CD3⁺CD4⁺ and CD3⁺CD8⁺ T cell populations. (**C**) The absolute CD4⁺ and CD8⁺ T cell counts in blood from healthy individuals (n = 14) and B-ALL patients (n = 30) are shown. Mann-Whitney U test was used for statistical analysis. (**D**) The percentages of T_N, T_{CM}, and $T_{EM/EMRA}$ cells in the CD3⁺CD4⁺ T cell population are shown. (**E**) The percentages of T_N, T_{CM}, and $T_{EM/EMRA}$ cells in the CD3⁺CD8⁺ T cell population are shown.

cells/µl, range 4–624 cells/µl; CD8⁺ median 76 cells/µl, range 9–458 cells/µl, n = 14) due to previous therapy and/or had circulating CD19⁺ blasts and had enrichment of CD8⁺ T cells without CD62L selection. The median CD3⁺CD8⁺ T cell purity after CD8⁺ selection was 84% (range 36.1%–95.7%, n = 12).

The selected CD4⁺ and CD8⁺ T cells were lentivirally transduced to express the CD19 CAR and a truncated human epidermal growth factor receptor (EGFRt) that enabled identification of transduced cells by flow cytometry using the anti-EGFR monoclonal antibody cetuximab. Transduced EGFRt⁺ CD4⁺ and CD8⁺ T cells were enriched during culture by a single stimulation with irradiated CD19⁺ lymphoblastoid cell line (LCL) (n = 27; Supplemental Figure 1, D and E). The median frequency of EGFRt⁺ CAR–T cells within the CD3⁺CD4⁺ and CD3⁺CD8⁺ subsets in the products at release for infusion was, respectively, 79.7% (range 50.0%–95.9%) and 84.2% (range 13.0%–95.6%). The infused CD3⁺CD4⁺EGFRt⁺ and CD3⁺CD8⁺EGFRt⁺ CAR–T cells were predominantly CD45RA⁻CD62L⁺ and CD45RA⁻CD62L⁻ (Supplemental Figure 2). CD8⁺EGFRt⁺ CAR–T cells that were manufactured from bulk CD8⁺ T cells contained a lower fraction of CD45RA⁻CD62L⁻ cells than those manufactured from CD8⁺ T_{CM} cells.

Assessment of toxicity following administration of CD19 CAR–T cells. The study was designed to evaluate the safety of 3 DLs (2×10^5/kg; 2×10^6/kg; and 2×10^7/kg) of CAR–T cells administered 48 to 96 hours after lymphodepleting chemotherapy. Serious acute toxicity in the first 2 hours after CAR–T cell infusion was not observed at any CAR–T cell dose. Patients developed the toxicities expected with cytotoxic chemotherapy, including BM suppression, alopecia, mild mucositis, and neutropenic fever. The most common toxicity that was observed in the first 14 days after CAR–T cell infusion was CRS, characterized by fever and/or hypotension and elevated serum levels of IL-6 and IFN-γ. Two patients died due to toxicity after CAR–T cell infusion: one developed severe CRS (sCRS) and multiorgan failure that was unresponsive to tocilizumab, etanercept, and corticosteroids, and another patient who developed transient sCRS died 122 days after CAR–T cell infusion with irre-

Table 1. Clinical characteristics of the treated patients

	Age (yr)	Prior therapy		BM blasts (% leukocytes) before lymphodepletion and CAR–T cell therapy	CD8+ T cell subset isolation	Lymphodepletion regimen	Infused CAR–T cells			BM response		
		Prior intensive therapies	Prior allogeneic HCT				CD4+EGFRt+ T cells/kg	CD8+EGFRt+ T cells/kg	Risk-adapted dosing for high tumor burden	Flow cytometry	Karyotyping, FISH, QPCR	IGH sequencing (copies/million nucleated cells)
1[A]	37	2	N	0.016	CD8TCM	CE	1×10^5	1×10^5	NA	MRD	Karyotyping, FISH negative, p210 QPCR positive	Not done
2	50	4	DUCB	0.65	CD8TCM	CE	1×10^6	1×10^6	NA	Negative	Karyotyping, FISH negative	0
3	32	3	MRelD	1.6	CD8TCM	Cy	1.97×10^6	3×10^4	NA	MRD	Karyotyping negative, p210 QPCR positive	Not done
4	71	2	N	16.5	CD8TCM	Cy	1×10^7	1×10^7	NA	Negative	Not done	Not done
5	28	4	N	4.8	CD4/14/45RA-neg	Cy	1×10^6	1×10^6	NA	Negative	Karyotyping, FISH negative, p210 QPCR positive	Not done
6[B]	48	2	N	31.8	CD8TCM	Cy	1.16×10^7	8.4×10^6	No	Not done	Not done	Not done
7	24	3	N	97	CD4/14/45RA-neg	Cy	1×10^5	1×10^5	Yes	Negative	Karyotyping, FISH, QPCR negative	9
8	37	4	MURD	83.6	CD8TCM	Cy	1×10^5	1×10^5	Yes	Negative	Karyotyping, FISH negative	Not done
9	37	2	N	30.2	CD8TCM	Cy	1×10^5	1×10^5	Yes	Negative	Karyotyping, FISH negative	0
10	58	3	MURD	7.9	CD8TCM	Cy	1×10^5	1×10^5	Yes	Negative	Karyotyping, FISH negative	0
11[C]	62	3	N	46	CD8TCM	Cy	1×10^5	1×10^5	Yes	Negative	Karyotyping, FISH negative	24
12	24	2	N	60.7	CD8	Cy	1×10^6	1×10^6	No	Negative	Karyotyping negative	Polyclonal
13	29	1	N	10	CD8	Cy	1.49×10^6	5.1×10^5	NA	Negative	Karyotyping negative	0
14	40	3	N	12.7	CD8TCM	Cy/Flu5	1×10^6	1×10^6	NA	Negative	Karyotyping, FISH negative	0
15[D]	52	3	N	87.2	CD8	Cy/Flu5	1×10^6	1×10^6	No	Negative	Abnormal karyotype, FISH positive	19507
16	22	1	N	23.5	CD8TCM	Cy/Flu5	1×10^6	1×10^6	No	Negative	Karyotyping negative	0
17[E]	52	5	N	49.6	CD8	Cy/Flu3	1×10^6	1×10^6	No	Negative	Karyotyping negative	0
18[A]	38	4	MRelD	10.7	CD8TCM	Cy/Flu3	1×10^6	1×10^6	NA	Negative	Karyotyping, FISH negative	5
19	39	3	MURD	28	CD8TCM	Cy/Flu3	1×10^6	1×10^6	No	Negative	Karyotyping negative	Polyclonal
20	51	3	N	1.1	CD8TCM	Cy/Flu5	1×10^6	1×10^6	NA	Negative	Karyotyping negative	0
21	30	2	N	17.4	CD8	Cy/Flu5	1×10^5	1×10^5	Yes	Negative	Karyotyping negative	Polyclonal
22	52	6	MURD; MURD	0.04	CD8	Cy/Flu3	1×10^5	1×10^5	NA	Negative	Not done	Not done
23	23	6	MURD	0.55	CD8TCM	Cy/Flu3	1×10^5	1×10^5	NA	Negative	FISH negative	2
24	38	2	N	0.014	CD8	Cy/Flu3	1×10^6	1×10^6	NA	Negative	FISH negative	Polyclonal
25	40	1	N	21	CD8TCM	Cy/Flu3	1×10^5	1×10^5	Yes	Negative	p190 QPCR negative	0
26	73	4	N	0.03	CD8	Cy/Flu3	1×10^6	1×10^6	NA	Negative	Karyotyping, FISH negative	Polyclonal
27	43	4	MURD	0	CD8TCM	Cy/Flu3	1×10^6	1×10^6	NA	Negative	Karyotyping negative	Not done
28	43	11	MRelD; Rel Haplo	28.6	CD8TCM	Cy/Flu3	1×10^5	1×10^5	Yes	Negative	p190 QPCR negative	0
29[F]	61	1	N	28.4	CD8	Cy/Flu3	1×10^5	1×10^5	Yes	Negative	Karyotyping, FISH negative	178
30	20	4	MURD	74.7	CD8	Cy/Flu3	1×10^5	1×10^5	Yes	Negative	FISH negative	9

N, none; DUCB, double umbilical cord blood; MURD, matched unrelated donor; MRelD, matched related donor; Rel Haplo, related haploidentical; CD4, CD4-positive immunomagnetic selection; CD4/14/45RA-neg, PBMCs depleted of CD4+, CD14+, and CD45RA+ cells; CD8TCM, PBMCs depleted of CD4+, CD14+, and CD45RA+ cells and selected for CD62L+ cells; Cy, 2–4 g/msq Cy; CE, Cy 2–4 g/msq and etoposide 100 mg/msq × 3; Cy/Flu3, Cy 30–60 mg/kg × 1 and Flu 25 mg/msq × 3; Cy/Flu5, Cy 30–60 mg/kg × 1 and Flu 25 mg/msq × 5; MRD, < 5% blasts by flow cytometry. [A]Patient 1 underwent allogeneic HCT after receiving CAR–T cells. After HCT, she relapsed and was reenrolled on the trial as patient 18. [B]Died on day 3 after CAR–T cell infusion due to sCRS. [C]PET indeterminate. [D]Subsequent relapse with phenotype switch to myeloid leukemia. [E]Died on day 122 in CR with irreversible neurotoxicity. [F]Day 28, MRD (0.08%) by flow and IGH sequencing (178 copies/million); day 42, MRD (0.007%) by flow; day 83, CR by flow, karyotype, FISH. No antileukemic treatment was given in the interim.

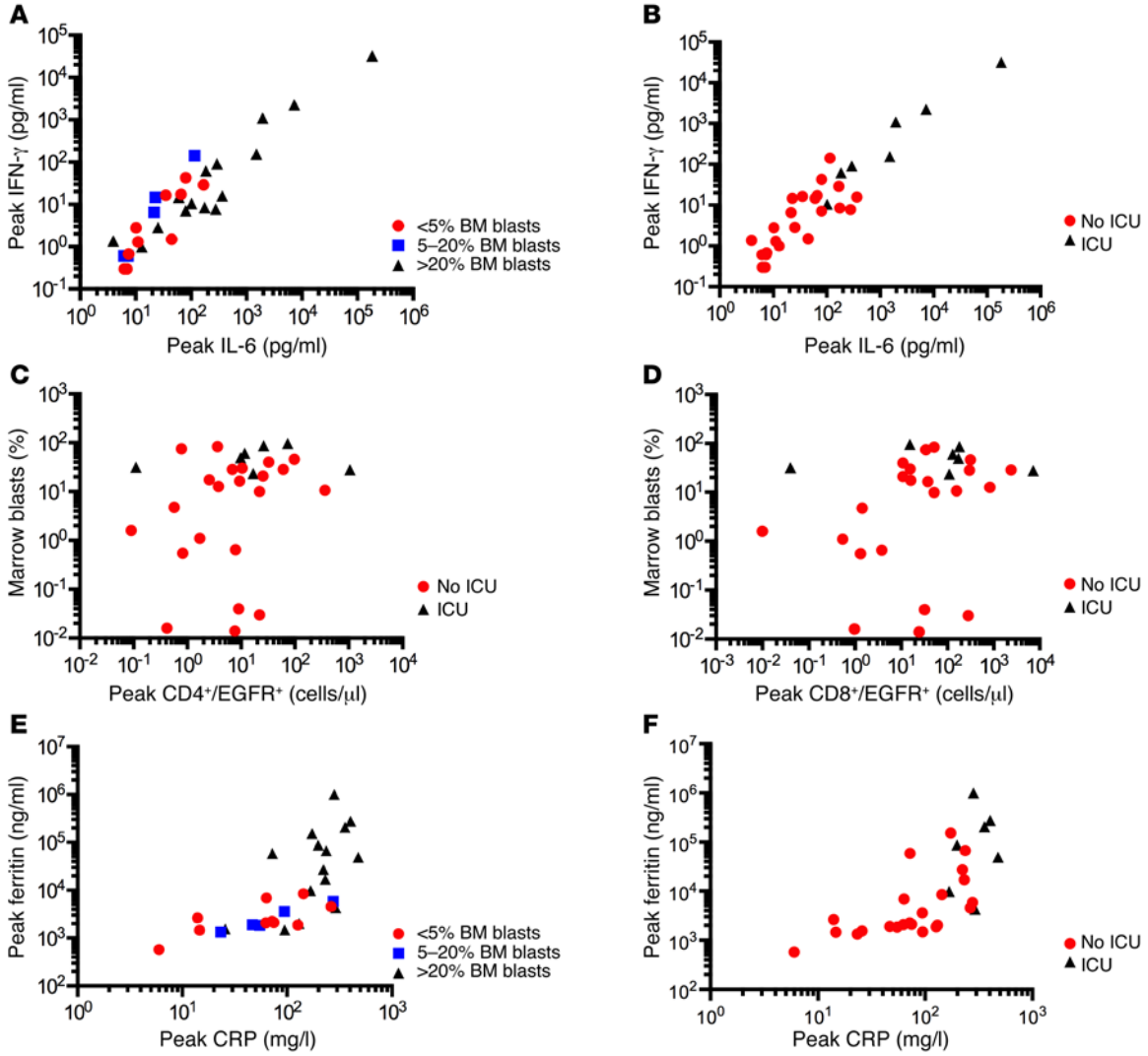

Figure 2. Serious toxicity due to CRS is mainly seen in B-ALL patients with high BM-tumor burden. (**A**) The peak IFN-γ and IL-6 concentrations in serum in the first 28 days after CAR–T cell infusion are shown in patients who had high (> 20% blasts; n = 15), intermediate (5%–20% blasts; n = 5), or low (≤ 5% blasts; n = 10) tumor burden before lymphodepletion chemotherapy and CAR–T cell infusion. Each point represents data from 1 patient. (**B**) The peak IFN-γ and IL-6 concentrations in serum in the first 28 days after CAR–T cell infusion are shown in patients who did (n = 7) or did not (n = 23) require ICU care. (**C** and **D**) The percentages of BM blasts before lymphodepletion chemotherapy and the peak absolute $CD3^+CD4^+$ (**C**) and $CD3^+CD8^+$ (**D**) $EGFRt^+$ CAR–T cell counts in the first 28 days after CAR–T cell infusion are shown in patients who did (n = 7) or did not (n = 23) require ICU care after CAR–T cell infusion. (**E**) The peak ferritin and CRP concentrations in serum in the first 28 days after CAR–T cell infusion are shown in patients who had high (> 20% blasts; n = 15), intermediate (5%–20% blasts; n = 5), or low (≤ 5% blasts; n = 10) tumor burden before lymphodepletion chemotherapy and CAR–T cell infusion. (**F**) The peak ferritin and CRP concentrations in serum in the first 28 days after CAR–T cell infusion are shown in patients who did (n = 7) or did not (n = 23) require ICU care.

versible neurologic toxicity. The first 2 patients treated at dose-level 3 (DL3) developed severe toxicities, including one of the patients who died. DL3 was therefore deemed too toxic, and no further patients were treated at this DL. Overall, 25 of 30 patients developed CRS between 6 hours and 9 days after CAR–T cell infusion, and 7 of these 25 patients had sCRS requiring ICU care. Of the 28 patients treated at DL1 and DL2, dexamethasone alone (n = 3) or with tocilizumab (n = 7) was used to treat CRS, resulting in prompt resolution of fever and hypotension in all patients (Supplemental Table 1).

Severe neurotoxicity (National Cancer Institute [NCI] common terminology criteria for adverse events [CTCAE] v4.03 grade ≥ 3) occurred in 15 of 30 patients either concurrent with or after the resolution of CRS. No patients developed grade 1 to 2 neurotoxicity. The clinical presentation of neurotoxicity was variable and manifested as mild to severe encephalopathy, focal neurologic deficits, and in 3 patients, generalized seizures. Five patients with grade of 3 or higher neurotoxicity developed transient disseminated intravascular coagulation. With the exception of one patient who developed severe irreversible neurologic deficits and subsequently died 122 days after CAR–T cell infusion, the neurologic symptoms and signs completely resolved over days to weeks.

Depletion of normal $CD19^+$ B cells, consistent with the in vivo presence of functional CD19 CAR–T cells, was noted in 29 of 29 patients on or before day 28, but hypogammaglobulinemia and late opportunistic infections were not prominent during the period

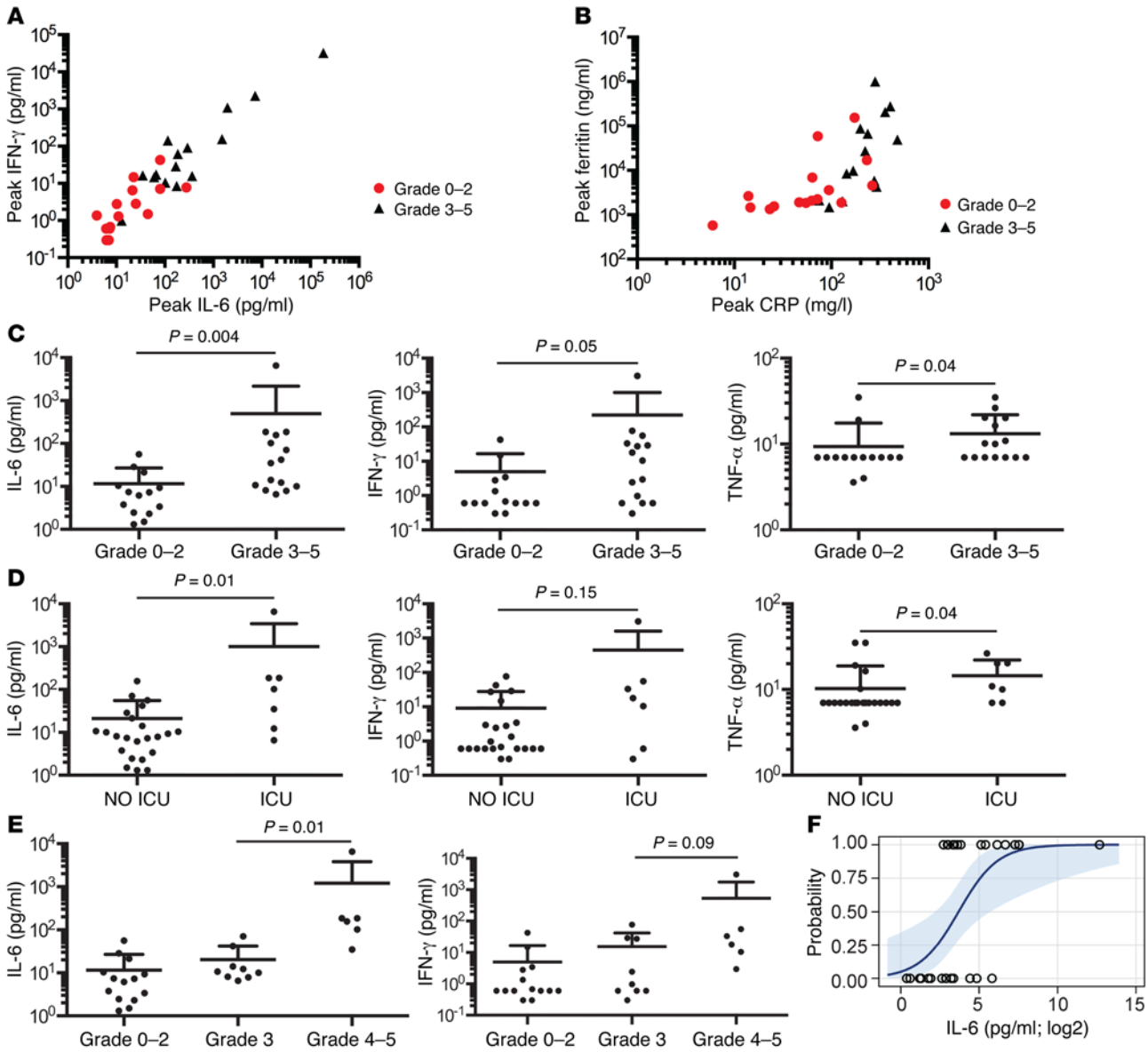

Figure 3. Relationship between serum cytokine, ferritin, and CRP levels and severe neurotoxicity. (**A**) The peak IL-6 and IFN-γ concentrations in serum in the first 28 days after CAR–T cell infusion in patients who developed NCI CTCAE grade 3 or higher neurotoxicity (n = 15) compared with those without neurotoxicity (n = 15). (**B**) The peak ferritin and CRP concentrations in serum in the first 28 days after CAR–T cell infusion in patients who developed NCI CTCAE grade 3 or higher neurotoxicity (n = 15) compared with those without neurotoxicity (n = 15). (**C**) Serum IL-6, IFN-γ, and TNF-α concentrations on day 1 after CAR–T cell infusion in patients who subsequently developed grade 3 to 5 neurotoxicity compared with those without neurotoxicity. Data represent the mean ± SEM. The Mann-Whitney U test was used for statistical analysis. (**D**) Serum IL-6, IFN-γ, and TNF-α concentrations on day 1 after CAR–T cell infusion in patients who subsequently required ICU care compared with those who did not require ICU care. Data represent the mean ± SEM. The Mann-Whitney U test was used for statistical analysis. (**E**) Serum IL-6 and IFN-γ concentrations on day 1 after CAR–T cell infusion in patients who subsequently developed the indicated grades of neurotoxicity. Data represent the mean ± SEM. (**F**) Predicted probability curve with bounding 95% CI limits showing the relationship between $\log_2$-transformed serum IL-6 concentration on day 1 after CAR–T cell infusion and the occurrence of grade 3 or higher neurotoxicity. Circles, observed; line, predicted.

of follow-up. A difference in the rate or severity of toxicity in the 11 patients with a prior allogeneic HCT was not apparent. CAR–T cells were manufactured from the engrafted donor T cells obtained from the patients after transplant, and it is notable that none of the 11 patients developed acute graft-versus-host disease (GVHD) after CAR–T cell therapy. One patient who had stage 1 acute skin GVHD before study enrollment developed chronic GVHD requiring corticosteroid therapy 3 months after CAR–T cell infusion.

Correlates of CRS and neurotoxicity. CRS is initiated by activation and proliferation of CAR–T cells after recognition of CD19$^+$ target cells and is characterized by elevated serum levels of IL-6 and IFN-γ (2). We observed significantly higher peak IL-6 and IFN-γ levels after CAR–T cell infusion in patients with high BM tumor burden (Figure 2A) and in those requiring ICU care compared with those that did not (Figure 2B), and the need for ICU correlated with a higher percentage of BM blasts before lym-

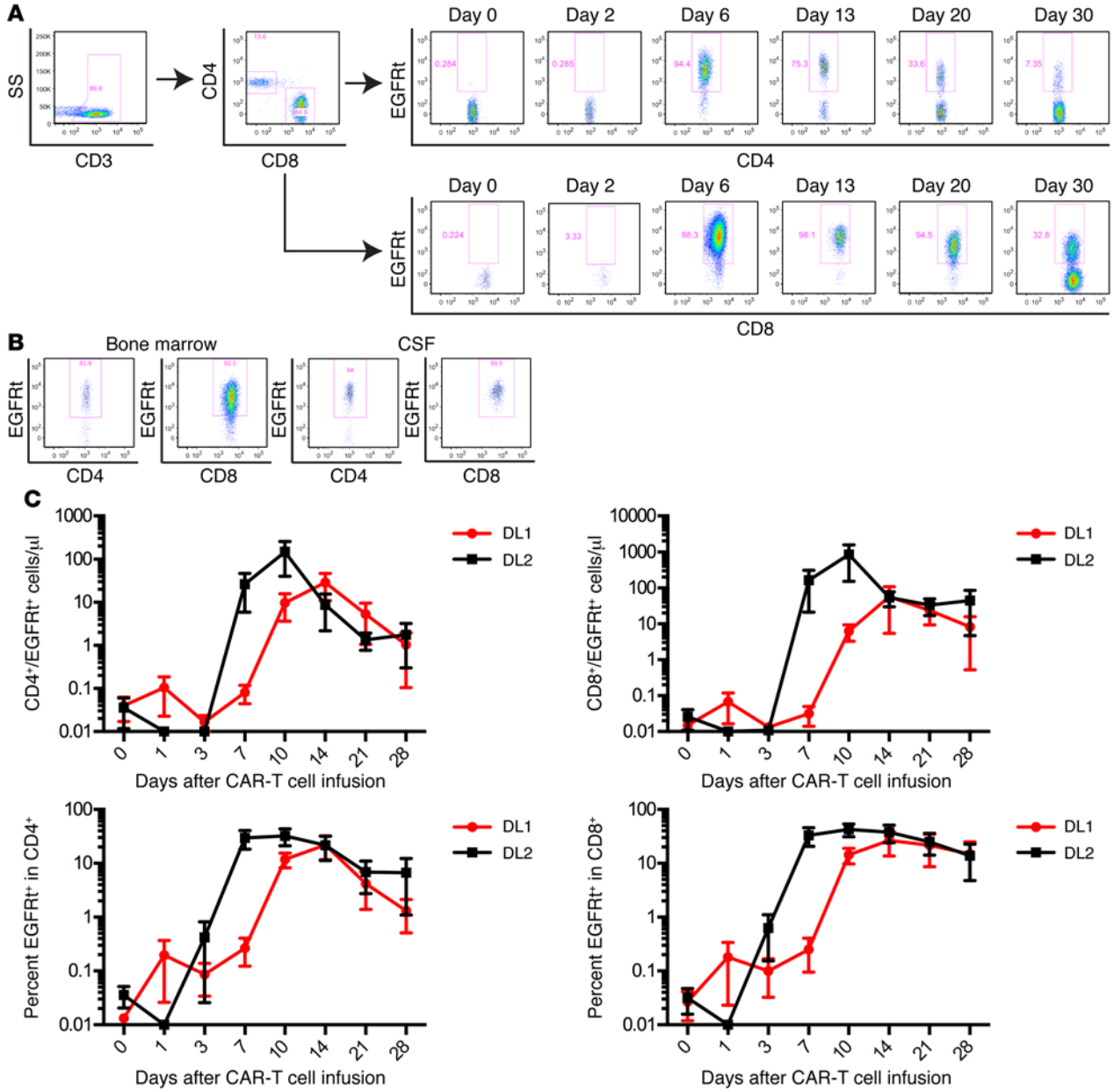

Figure 4. Kinetics of CAR–T cell expansion, migration, and peak blood levels in relation to cell dose. (**A**) Flow cytometry plots showing EGFRt$^+$ CAR–T cells detected in the CD3$^+$CD4$^+$ and CD3$^+$CD8$^+$ T cell subsets in blood of a representative B-ALL patient at the indicated times after CAR–T cell infusion. (**B**) EGFRt$^+$ CD4$^+$ and CD8$^+$ CAR–T cells infiltrate the BM and CSF. A representative flow cytometry analysis of a BM and CSF sample from 1 patient is shown. (**C**) Graphs show the absolute count (top) and percentage (bottom) of EGFRt$^+$ CAR–T cells in the CD3$^+$CD4$^+$ (left) and CD3$^+$CD8$^+$ (right) T cell subsets in blood at intervals after CAR–T cell infusion in patients treated at DL1 (n = 6) or DL2 (n = 12) prior to incorporation of risk-adjusted CAR–T cell dosing. Data represent the mean ± SEM.

phodepletion chemotherapy (Figure 2, C and D). We used flow cytometry to identify EGFRt$^+$ CAR–T cells and determine their frequency in peripheral blood obtained at prescribed intervals after infusion. With the exception of the patient who died on day 3 after CAR–T cell infusion prior to peak CAR–T cell expansion, no patients with a peak CD4$^+$ EGFRt$^+$ CAR–T cell count of less than 9.8 cells/μl or CD8$^+$ EGFRt$^+$ count of less than 15 cells/μl required ICU care, whereas 6 of 15 (40%) patients with a peak CD4$^+$ EGFRt$^+$ count of 9.8 or more cells/μl and 6 of 21 (29%) with a peak CD8$^+$ EGFRt$^+$ count of 15 or more cells/μl required ICU. Elevations of serum C-reactive protein (CRP) and ferritin, which are more readily measured by clinical laboratories than serum cytokines, also correlated with BM disease burden (Figure 2E) and with the occurrence of sCRS requiring ICU care (Figure 2F). sCRS was more likely to occur in patients with peak CRP concentrations of 150 or more mg/l (7 of 13) and/or with serum ferritin concentrations of 10,000 or more ng/ml (5 of 10). Ferritin and CRP levels declined after tocilizumab or corticosteroid therapy.

The pathogenesis of neurotoxicity developing after CD19 CAR–T cell therapy is poorly defined. In our study, all patients who developed neurotoxicity had evidence of CRS, and peak levels of IL-6, IFN-γ, ferritin, and CRP were significantly higher

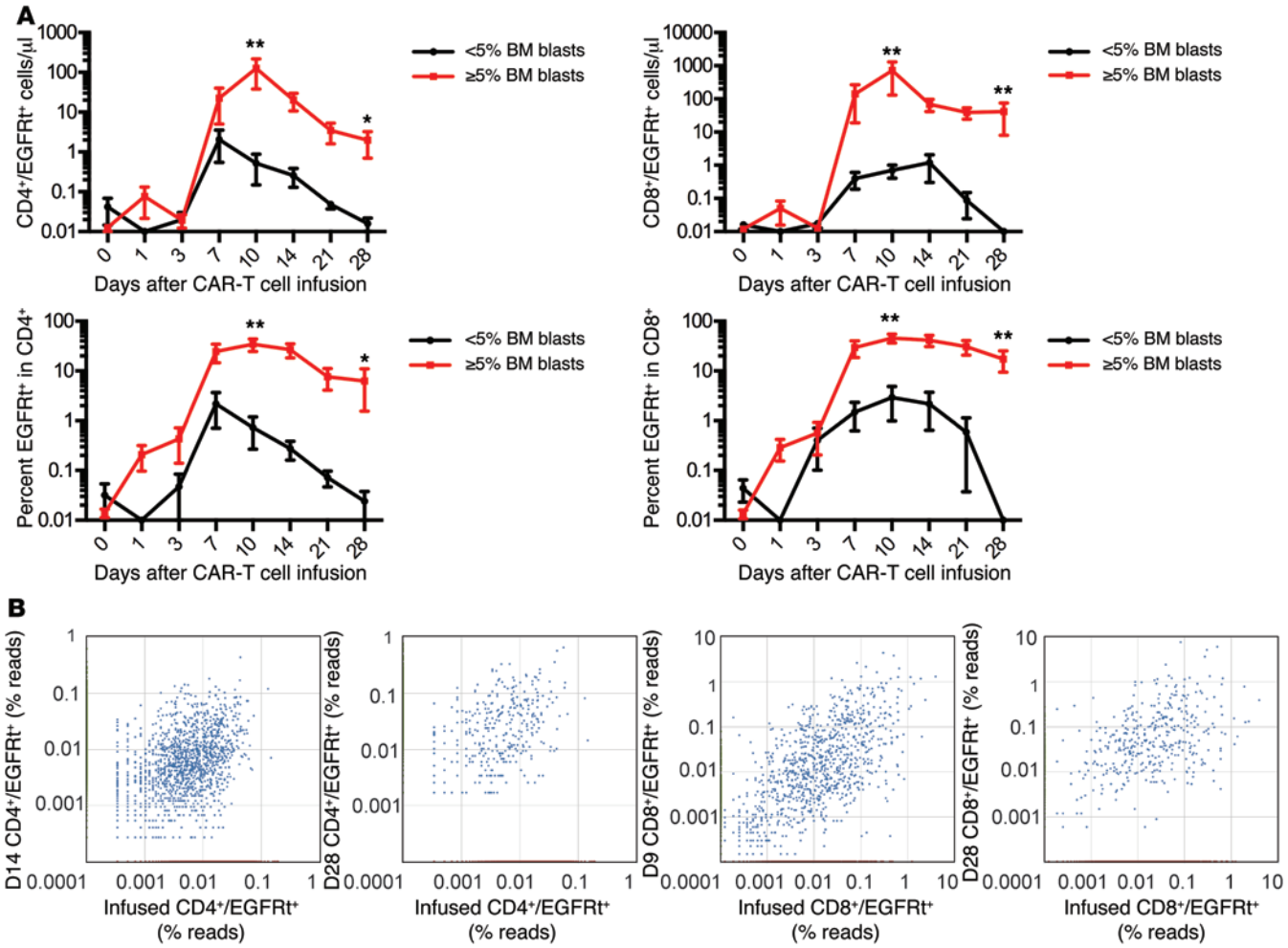

Figure 5. CAR–T cells are detected at higher levels in blood from patients with high tumor burden. (**A**) The graphs show the absolute count (top) and percentage (bottom) of EGFRt+ CAR–T cells in the CD3+CD4+ (left) and CD3+CD8+ (right) T cell subsets in blood at intervals after CAR–T cell infusion in patients with high (≥ 5% BM blasts by flow cytometry; $n = 15$) or low (< 5% BM blasts by flow cytometry; $n = 5$) BM disease burden prior to incorporation of risk-adjusted CAR–T cell dosing. Data represent the mean ± SEM. The Mann-Whitney U test was used for statistical analysis. *$P < 0.05$; **$P < 0.01$. (**B**) ImmunoSEQ analysis of the TCRB genes of CAR–T cells sorted from blood of treated patients demonstrates polyclonality of CD4+ (left) and CD8+ (right) CAR–T cells in the recipient after adoptive transfer and sharing of sequences between the infusion product and the recipient after adoptive transfer. Each point represents 1 detected TCRB gene sequence. The axes indicate the percentage of TCRB reads. TCRB sequences identified by points in red were detected only in the infused CAR–T cell product (x axes). TCRB sequences identified by points in green are detected only in the recipient at the indicated day after CAR–T cell infusion (y axes). TCRB sequences identified by points in blue are detected both in the infused CAR–T cell product and in the recipient at the indicated day after infusion.

in patients who developed grade 3 or higher neurotoxicity (Figure 3, A and B). The fever and hypotension that accompany CRS were responsive to administration of corticosteroids and/or tocilizumab, but neurotoxicity was less responsive to these interventions. We evaluated serum levels of IL-6, IFN-γ, and TNF-α on the first day after CAR–T cell infusion to determine whether these might serve as biomarkers to identify patients at high risk for subsequent neurotoxicity and ICU care. We found that IL-6, IFN-γ, and TNF-α levels on the first day after CAR–T cell infusion were significantly higher in patients who subsequently developed severe (grade ≥ 3) neurotoxicity compared with those who did not (Figure 3C) and were also higher in patients who required ICU care (Figure 3D). Moreover, serum IL-6 and IFN-γ concentrations on day 1 after CAR–T cell infusion were significantly higher in patients who subsequently developed grade 4 neurotoxicity compared with patients who developed grade 3 neurotoxicity (Figure 3E). Univariate logistic analysis suggested that IL-6 concentration is a predictor of patients who are likely to develop grade 3 or higher neurotoxicity (odds ratio 11.0 [95% CI: 1.4–84.3], $P = 0.02$) (Figure 3F). Stepwise multivariate logistic regression analysis incorporating day 1 serum IL-6 concentration, infused CAR–T cell dose, lymphodepletion chemotherapy regimen, and the fraction of BM represented by normal and abnormal CD19+ cells indicated that serum IL-6 concentration of more than 30 pg/ml on day 1 ($P = 0.02$) and the total number of CD19+ cells in BM before therapy ($P = 0.06$) are independent predictors of subsequent development of grade 3 or higher neurotoxicity. Of note, serum IL-6 of more than 30 pg/ml on day 1 identified all patients in our study who subsequently developed grade 4 or higher neurotoxicity. Thus, evaluation of serum IL-6

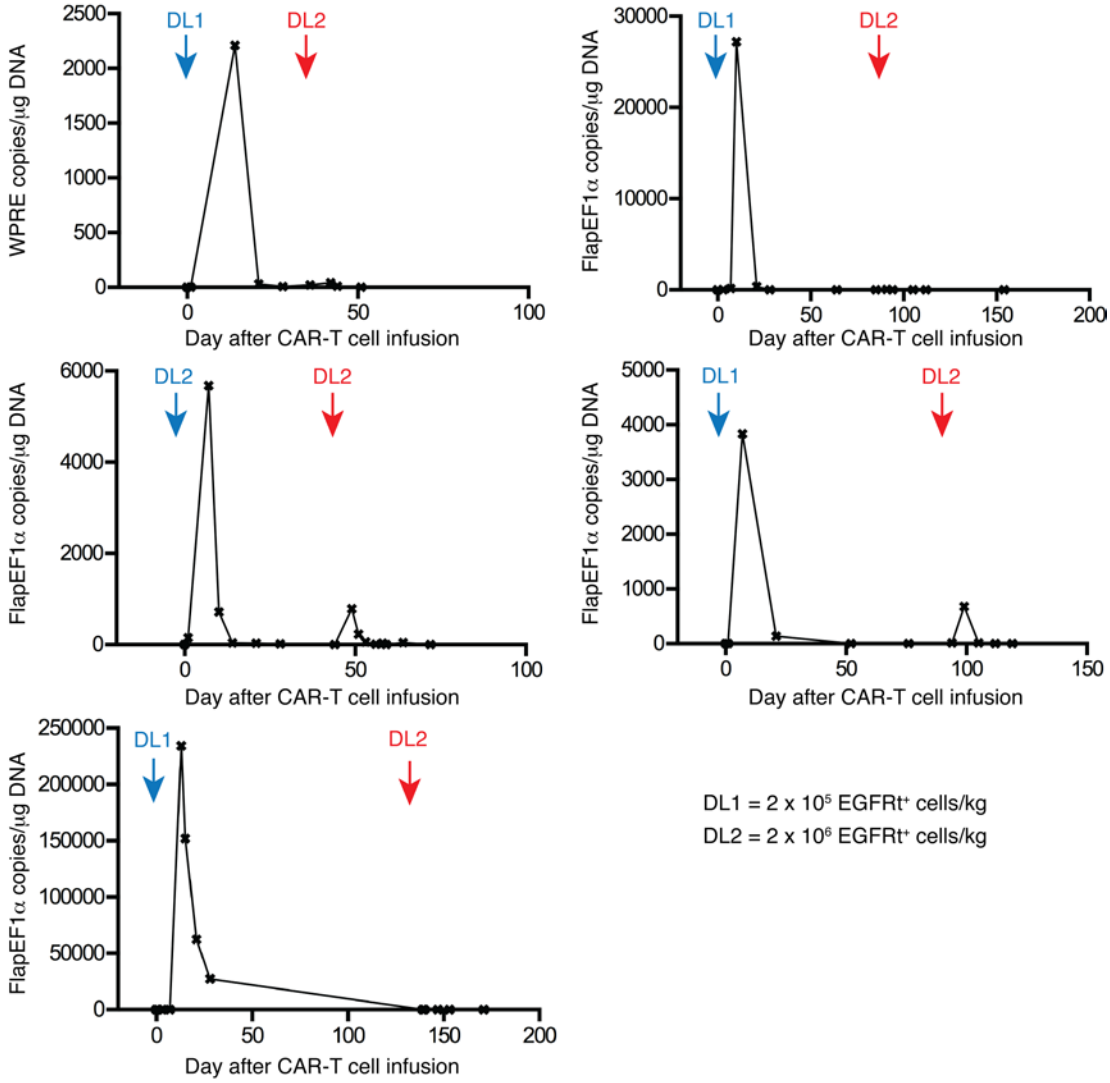

Figure 6. Failure to achieve engraftment of CAR–T cells after second infusions. Patients who had persistent MRD after the first CAR–T cell infusion or subsequently relapsed after attaining a CR (n = 5) received a second infusion of CAR–T cells at an equivalent (n = 1) or 10-fold higher EGFRt⁺ dose (n = 4) compared with their first infusion. Engraftment after each infusion was analyzed by QPCR to detect a transgene vector sequence. Each graph shows the number of copies of integrated transgene (WPRE copies/μg DNA, n = 1; FlapEF1α copies/μg DNA, n = 4) detected in PBMCs collected at the indicated times after the first and second CAR–T cell infusions. The times and doses of the first (blue) and second (red) CAR–T cell infusions are noted on the graphs.

concentration early after CAR–T cell infusion might be used to identify patients at high risk of severe neurotoxicity to evaluate early intervention approaches.

Because the occurrence of toxicity correlated with BM tumor burden and sCRS was noted in patients treated at a higher CAR–T cell dose, we initiated risk-adapted CAR–T cell dosing during the course of the study, in which patients with greater than 20% BM blasts received a low dose of CAR–T cells (2×10^5 EGFRt⁺ cells/kg) and those with 20% or less BM blasts received a higher dose of CAR–T cells (2×10^6 EGFRt⁺ cells/kg). Prior to incorporation of risk-adapted CAR–T cell dosing, 6 of 6 patients with high–tumor burden B-ALL who were treated at DL2 or DL3 ($\geq 2 \times 10^6$ EGFRt⁺ cells/kg) required ICU care after CAR–T cell therapy, and all 6 patients developed severe neurotoxicity (median grade 4). In contrast, only 1 of 10 patients with high–tumor burden B-ALL who were treated with risk-adapted dosing at DL1 required ICU care, and only 5 of 10 developed neurotoxicity (median grade 3).

In vivo expansion and persistence of CD19 CAR–T cells. The proliferation, migration to sites of tumor, and persistence of CAR–T cells in vivo after adoptive transfer are likely to be critical determinants of antitumor efficacy, and the kinetics of CAR–T cell expansion may in part dictate the risk of serious toxicity. CAR–T cells were detected by flow cytometry in the blood at 1 or more time points after infusion in all patients (Figure 4A). CAR–T cells were also present in BM obtained at response evaluation in 22 of 27 patients from whom the BM was examined for the presence of CAR–T cells and in the CSF of 6 of the 8 patients from whom samples were obtained for clinical indications (Figure 4B).

Several factors could contribute to CAR–T cell expansion and persistence in vivo, including cell product composition, cell dose, tumor burden, and the conditioning regimen used to provide lymphodepletion. Previous studies at other centers in which CD19 CAR–T cells were manufactured from T cells of undefined composition did not identify a clear correlation between the

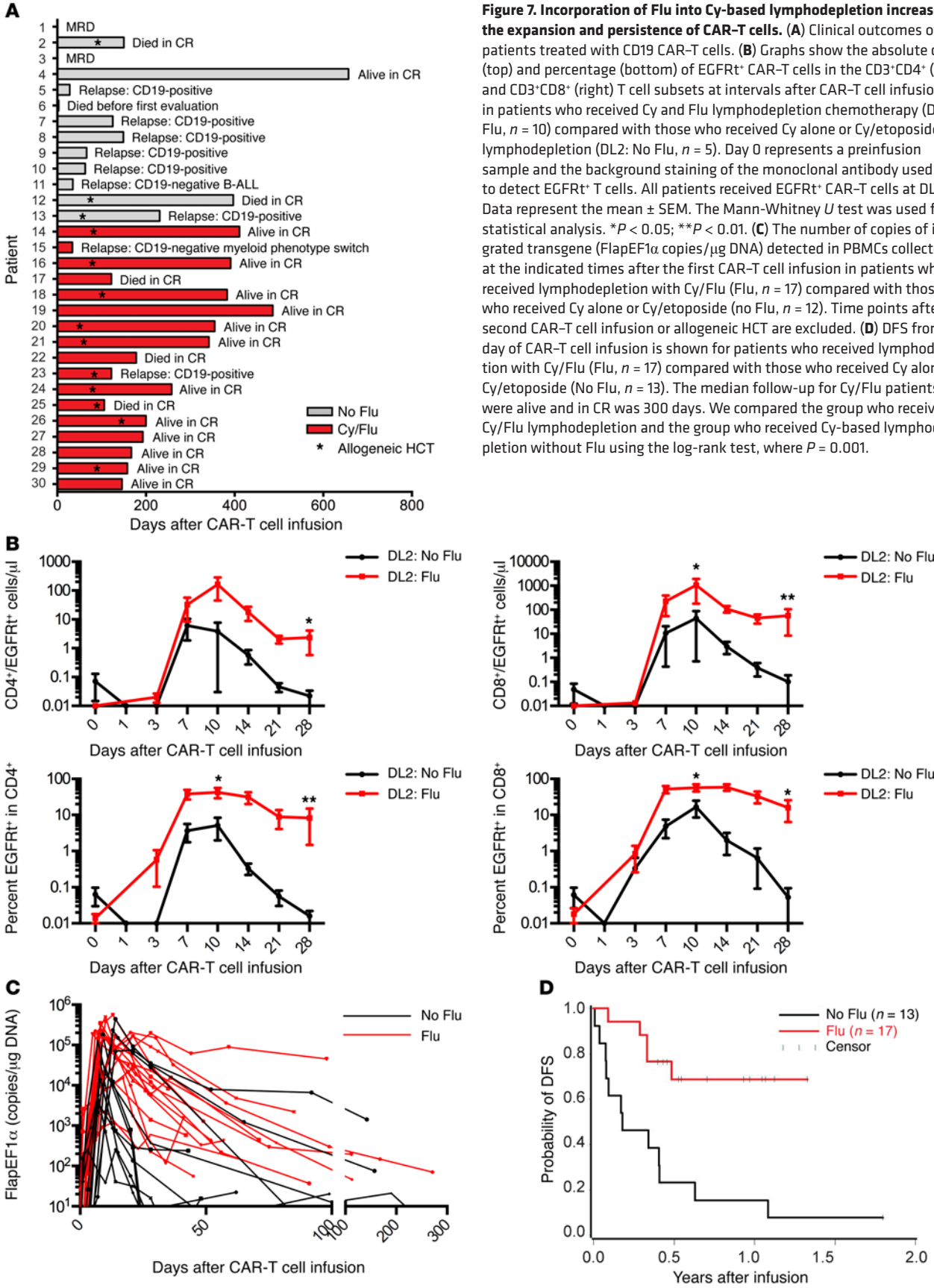

Figure 7. Incorporation of Flu into Cy-based lymphodepletion increases the expansion and persistence of CAR–T cells. (**A**) Clinical outcomes of patients treated with CD19 CAR–T cells. (**B**) Graphs show the absolute count (top) and percentage (bottom) of EGFRt$^+$ CAR–T cells in the CD3$^+$CD4$^+$ (left) and CD3$^+$CD8$^+$ (right) T cell subsets at intervals after CAR–T cell infusion in patients who received Cy and Flu lymphodepletion chemotherapy (DL2: Flu, n = 10) compared with those who received Cy alone or Cy/etoposide lymphodepletion (DL2: No Flu, n = 5). Day 0 represents a preinfusion sample and the background staining of the monoclonal antibody used to detect EGFRt$^+$ T cells. All patients received EGFRt$^+$ CAR–T cells at DL2. Data represent the mean ± SEM. The Mann-Whitney U test was used for statistical analysis. *$P < 0.05$; **$P < 0.01$. (**C**) The number of copies of integrated transgene (FlapEF1α copies/µg DNA) detected in PBMCs collected at the indicated times after the first CAR–T cell infusion in patients who received lymphodepletion with Cy/Flu (Flu, n = 17) compared with those who received Cy alone or Cy/etoposide (no Flu, n = 12). Time points after a second CAR–T cell infusion or allogeneic HCT are excluded. (**D**) DFS from the day of CAR–T cell infusion is shown for patients who received lymphodepletion with Cy/Flu (Flu, n = 17) compared with those who received Cy alone or Cy/etoposide (No Flu, n = 13). The median follow-up for Cy/Flu patients who were alive and in CR was 300 days. We compared the group who received Cy/Flu lymphodepletion and the group who received Cy-based lymphodepletion without Flu using the log-rank test, where P = 0.001.

infused CAR–T cell dose and the absolute number of CAR–T cells detected in vivo in the recipient (2–4). We found that administering a consistent CAR–T cell product of a defined $CD4^+$:$CD8^+$ T cell ratio to all patients revealed a relationship between cell dose and the peak number of $CD4^+$ and $CD8^+$ CAR–T cells. Prior to commencing risk-adapted CAR–T cell dosing based on BM tumor burden, we found that patients who received CAR–T cells at DL2 had an earlier and higher peak in absolute $CD4^+$ and $CD8^+$ $EGFRt^+$ CAR–T cell counts in blood compared with those who received DL1 (Figure 4C). At both DLs, the absolute number of $CD8^+$ CAR–T cells was higher than that of $CD4^+$ CAR–T cells at the peak of expansion, despite $CD4^+$ and $CD8^+$ CAR–T cells having been infused at the same dose.

The burden of $CD19^+$ cells in the patient could also affect CAR–T cell numbers either by inducing their proliferation or resulting in activation-induced cell death. Stratifying patients treated prior to risk-adapted dosing based on the proportion of $CD19^+$ leukemia blasts in the BM showed that patients with a higher percentage of blasts in the BM had significantly higher $CD4^+$ and $CD8^+$ CAR–T cell counts in the blood at the peak of expansion and better persistence at day 28 after infusion (Figure 5A). The accumulation of $CD4^+$ and $CD8^+$ CAR–T cells in vivo could occur as a result of expansion of a diverse repertoire of polyclonal T cells derived from the transduced T cell population or the expansion of few highly proliferative T cell clonotypes with a proliferative and/or survival advantage. To distinguish these possibilities, we performed high-throughput sequencing of the T cell receptor β (TCRB) genes utilized by flow-sorted $CD4^+$ and $CD8^+$ $EGFRt^+$ CAR–T cells obtained from the infused CAR–T cell products of 5 patients, at the peak of CAR–T cell expansion in vivo, and at one or more later time points. Both at the peak of expansion and at later times after elimination of detectable leukemia, the $CD4^+$ and $CD8^+$ CAR–T cells present in vivo were polyclonal, and multiple distinct TCRB clonotypes that were identified in the infusion product were observed in the CAR–T cell population in the patient (Figure 5B). Together, these results demonstrate that the infusion of CAR–T cell products comprising $CD8^+$ and $CD4^+$ T cells in a defined ratio results in predictable polyclonal proliferation of both $CD4^+$ and $CD8^+$ T cells with kinetics that are affected by both CAR–T cell dose and tumor burden.

Clinical response. Twenty-nine of 30 patients who received CAR–T cells survived for more than 21 days and were evaluated for disease response by BM aspirate and biopsy. All patients (100%) had no detectable leukemia in the BM by morphology, and in 27 of 29 patients (93%), leukemia was undetectable by high-resolution flow cytometry (Table 1). Of the 27 patients who achieved BM remission by flow cytometry, one initially had minimal residual disease (MRD) by flow cytometry at a level of 0.08% identified on day 28 after CAR–T cell infusion; however, in the absence of any additional antileukemic therapy, a subsequent BM biopsy on day 83 after CAR–T cell infusion showed no evidence of disease by flow cytometry, karyotyping, or FISH studies using probes that were informative for the patient's disease. The 2 patients who did not achieve remission by flow cytometry had a low level (< 5%) of abnormal BM blasts by flow cytometry before CAR–T cell infusion. One of these patients received a cell product with a $CD4^+$:$CD8^+$ CAR–T cell ratio of 66:1 due to failure of the $CD8^+$ T cells selected from this patient to expand in culture. The other patient had 0.016% abnormal BM blasts by flow cytometry before CAR–T cell infusion, received CAR–T cells at DL1, and had poor in vivo CAR–T cell expansion (peak $CD8^+$ $EGFRt^+$ 0.97/μl, peak $CD4^+$ $EGFRt^+$ 0.42/μl). This patient subsequently underwent allogeneic HCT, but relapsed after HCT and was reenrolled in the CAR–T cell study. The patient achieved a CR after being retreated with CAR–T cells that were manufactured from T cells collected from the patient after allogeneic HCT and administered at a higher dose (DL2).

Molecular studies of BM, including quantitative PCR (QPCR), FISH, and conventional karyotyping, were negative in all patients who achieved remission by flow cytometry and had an identified B-ALL–associated genomic mutation, except for 2 patients — one with a persistent t(4;11) who subsequently relapsed with a clonally related $CD19^-$ acute myeloid leukemia and a second patient with BCR-ABL transcripts identified at the limit of detection by QPCR (Table 1). Thus, 25 of 29 patients (86%) achieved CR without evidence of MRD by flow cytometry and conventional karyotyping, FISH, or QPCR in those with an identified B-ALL–associated genomic mutation. Deep sequencing of the immunoglobulin heavy locus (IGH) genes in BM samples from 17 patients in whom we identified a neoplastic clonal IGH sequence showed that 10 (59%) had no detectable disease using an assay with a sensitivity to detect 1 malignant blast in 1,000,000 nucleated cells. In addition to the efficacy in eliminating BM- and blood-based leukemic blasts, extramedullary disease identified by PET-CT scan was eliminated in 6 of 7 patients after CAR–T cell therapy (Supplemental Figure 3). We did not observe a difference in response rate between patients who had or had not previously undergone allogeneic HCT (HCT group, 10/11 CR, 1/11 BM MRD; no HCT group, 15/19 CR, 3/19 BM MRD, 1/19 died before evaluation), demonstrating that CD19 CAR–T cells of defined composition can be successfully manufactured and administered to patients following allogeneic HCT. Thus, the data show a high rate of CR with CAR–T cells of defined $CD4^+$:$CD8^+$ T cell ratio in patients with refractory B-ALL, including those with extramedullary disease or with leukemia relapse after allogeneic HCT.

Transgene immune responses limit persistence and efficacy of second CAR–T cell infusions. Five patients treated in our study with CAR–T cells after Cy-based lymphodepletion had persistent leukemia or subsequently relapsed and received a second infusion of CAR–T cells at the same (n = 1) or a 10-fold higher dose (n = 4) after no lymphodepletion (n = 1) or lymphodepletion with Cy and Flu (n = 3) or clofarabine (n = 1). Despite evidence of CAR–T cell proliferation after the first infusion and the same or higher BM blast count at the time of second infusion, there was no expansion or persistence of CAR–T cells or demonstrable antitumor activity in any of these 5 patients (Figure 6). We considered that these patients might have mounted a T cell immune response directed at epitopes encoded by the CAR transgene after the first infusion, since the CD19-specific single-chain variable fragment (scFv) is of murine origin and there are unique fusion sites between components of the CAR. To evaluate whether a cytotoxic $CD8^+$ T cell response to autologous CAR–T cells was present, we used a modification of an in vitro assay we previously reported to analyze transgene product immunogenicity (19, 20). We detected CAR-

specific T cell responses in all 5 patients in whom CAR–T cells failed to persist after the second infusion, and epitope mapping in 1 patient identified immunogenic epitopes within the murine FMC63 scFv (Supplemental Figure 4).

Addition of Flu to Cy lymphodepletion improves persistence of CAR–T cells. Ten of 12 patients (83%) who received lymphodepletion with Cy alone or with etoposide followed by CAR–T cell infusion and who survived until disease restaging achieved BM CR by flow cytometry. We observed recovery of endogenous B cells in 8 of these patients by day 90 after CAR–T cells, and 7 patients subsequently relapsed (Figure 7A). One of the patients relapsed with $CD19^-$ leukemia, but the remaining 6 relapses were $CD19^+$, suggesting a loss of CAR–T cell immunosurveillance. Indeed, in 5 of the 6 patients with $CD19^+$ relapse, a loss of CAR–T cell engraftment in blood was shown by PCR analysis for transgene sequences, and an immune response to the CAR transgene product was detected in all of these patients.

To determine whether the development of an immune response to CAR–T cells might be prevented or delayed by intensifying the lymphodepletion regimen, we administered Cy/Flu to 17 subsequent patients prior to CAR–T cell infusion and compared CAR–T cell expansion and persistence to those of prior patients who received Cy without Flu. Patients with similar BM blast percentage who received Cy/Flu and DL2 of CAR–T cells had a significantly higher peak of expansion and numbers of $CD4^+$ and $CD8^+$ $EGFRt^+$ CAR–T cells at day 28 than those treated at DL2 who did not receive Flu (Figure 7, B and C). Sixteen of 17 patients who received Cy/Flu lymphodepletion and DL1 or DL2 of CAR–T cells had a CR. Three of 4 patients who received lymphodepletion with Cy or Cy/etoposide and had no detectable disease by IGH sequencing ultimately relapsed, whereas 0 of 6 patients who received Cy/Flu lymphodepletion and eliminated the malignant clone by IGH sequencing relapsed. Although follow-up of the cohort of patients who received Cy/Flu lymphodepletion is short, the DFS of this group is superior to those that did not receive Flu (Figure 7D).

Discussion

Previous clinical trials have reported a high rate of morphologic remission in small numbers of adult and pediatric patients with B-ALL treated with CD19 CAR–T cells (2–4). This approach represents an important therapeutic advance; however, much remains to be learned regarding the optimal lymphodepletion regimens and cell dose(s) to eradicate MRD, the prediction and management of toxicities, and the mechanisms of relapse. Systematically studying these issues has been challenging in part because of the differences in the phenotypic composition of the CAR–T cell products that were administered to individual patients in prior trials (2–4). Our data show that heavily pretreated adult B-ALL patients have highly variable numbers and proportions of $CD4^+$ and $CD8^+$ T cell subsets in peripheral blood. Preclinical studies provide support for improving potency and predictability of therapeutic efficacy by manufacturing CD19 CAR–T cell products of defined $CD4^+$ and $CD8^+$ subset composition (17). Here, we describe what we believe is the first clinical trial that assesses the feasibility of selecting and engineering defined T cell subsets with a CD19 CAR and formulating a cell product of a defined ratio of $CD4^+$:$CD8^+$ CAR–T cells.

We enrolled 32 patients and, importantly, did not exclude any patient based on a low absolute lymphocyte count, the presence of circulating blasts, or the results of a screening test to ensure the patient had sufficient T cells capable of proliferating to CD3/CD28 stimulation. Therefore, our study was not biased due to exclusion of patients with poor lymphocyte numbers and function. A clinical trial of CD19 CAR–T cell therapy for pediatric B-ALL excluded 24% of patients due to the failure of T cells to meet predefined criteria for in vitro proliferation (21).

A primary objective of the study was to assess the feasibility of selecting $CD4^+$ and $CD8^+$ subsets for manufacturing of CAR–T cells and formulating the cell product in a consistent 1:1 ratio of $CD4^+$ and $CD8^+$ CAR–T cells. $CD8^+$ T_{CM} cells and their progeny have been shown to have stemness and to exhibit superior persistence compared with T_{EM} cells after adoptive transfer, suggesting a potential advantage of this subset for providing long-term persistence (12, 22). Our data show that in heavily pretreated B-ALL patients, the absolute $CD8^+$ T_{CM} counts were sufficient for selection and manufacturing of a CAR–T cell product in 16 of 30 patients and that selection of bulk $CD8^+$ T cells was feasible in the remaining 14 patients. Thus, a cell product comprising $CD4^+$ and $CD8^+$ CAR–T cells was successfully manufactured and infused to all patients with refractory B-ALL, and the 1:1 ratio of $CD4^+$:$CD8^+$ CAR–T cells was achieved in 27 of 30 patients.

The high overall rate of BM remission of 93% by flow cytometry in this study and differences in lymphodepletion regimens and infused cell doses do not allow comparison of the efficacy of CAR–T cell products manufactured from $CD8^+$ T_{CM} cells or from bulk $CD8^+$ T cells. Analysis of differences in long-term persistence of cell products that were selected for $CD8^+$ T_{CM} or bulk $CD8^+$ T cells in our study was further complicated by our findings that immune-mediated rejection of CAR–T cells occurs in some patients, which may provide an explanation for the loss of CAR–T cells observed in a subset of patients in other studies (1–4). Nevertheless, our data demonstrate that performing cell selections from heavily pretreated B-ALL patients is feasible and that formulating CD19 CAR–T cells in a defined $CD4^+$:$CD8^+$ CAR–T cell ratio, either from a starting population of isolated $CD8^+$ T_{CM} or bulk $CD8^+$ cells, can provide a remarkably effective CAR–T cell product at cell doses that are 5- to 100-fold lower than those used to treat a majority of patients in other trials (1–4). The 93% remission rate by flow cytometry and 86% MRD-negative CR rate in our study compares very favorably to that reported by others in which CAR–T cells of undefined composition were manufactured using CD19 CARs that incorporate either a 4-1BB costimulatory domain (children and young adults, 79%) or a CD28 costimulatory domain (adults, 75%; children and young adults, 60%) (1–4).

An important predictor of the efficacy of CD19 CAR–T cells is their ability to expand in vivo in response to recognition of $CD19^+$ target cells, and the patients that failed to respond in prior studies typically had poor accumulation of CAR–T cells in vivo. The infusion of CAR–T cell products comprising a uniform ratio of $CD4^+$:$CD8^+$ CAR–T cells demonstrated a correlation between cell dose and earlier and higher peak expansion of clonally diverse CAR–T cells, a finding that has not been reported in studies in which CAR–T cells were manufactured and infused without consideration of the $CD4^+$:$CD8^+$ ratio. Independent of cell dose,

tumor burden was an important factor in driving CAR–T cell expansion, and patients with 5% or greater BM blasts had on average a 100-fold greater expansion of both $CD8^+$ and $CD4^+$ CAR–T cells than patients with less than 5% blasts. Administering a single low dose of 2×10^5 CAR–T cells/kg of a defined $CD4^+$:$CD8^+$ T cell ratio was effective in inducing a CR in all patients with high BM tumor burden. The high potency of the CAR–T cell products was not limited to elimination of BM disease, and bulky extramedullary disease identified by PET/CT scan was also eradicated in all but 1 patient. Seven of 17 patients (41%) who achieved BM CR by flow cytometry had detectable copies of the neoplastic IGH sequence in BM early after CAR–T cell infusion; however, the detection of nonviable leukemic tissue renders the significance of this finding uncertain. Only 4 of these 7 patients subsequently relapsed; 2 of these had CD19-negative leukemia. Three patients had persistent BM disease detected by flow cytometry at the first evaluation after receiving CAR–T cells; 1 of these subsequently achieved CR in the absence of further therapy. Of the 2 patients who never achieved BM CR by flow cytometry, 1 received a predominantly $CD4^+$ CAR–T cell product because we were unable to propagate sufficient $CD8^+$ CAR–T cells in culture. The clinical outcome in this patient is consistent with our preclinical observations in Raji tumor–bearing immunodeficient mice that received CAR–T cells manufactured from distinct T cell subsets, showing reduced potency when either $CD8^+$ or $CD4^+$ CAR–T cells were omitted from the formulated product (17). Both of the remaining patients had low tumor burden in the BM before CAR–T cell therapy, raising the additional possibility that a higher dose of CAR–T cells may be necessary to effectively treat patients with low tumor burden, perhaps due to a stochastic failure to receive sufficient antigenic stimulation to drive CAR–T cell expansion in vivo. Given the high rate of CR in our phase I clinical trial, a larger patient cohort will need to be studied to understand the mechanisms responsible for failure to achieve remission.

Although CD19 CAR–T cells are therapeutically effective in patients with relapsed and refractory B-ALL, significant toxicities have occurred in all studies, highlighting the need to improve the therapeutic index (2–4, 23). In our study, severe toxicity due to CAR–T cells was predominantly seen in patients with 20% or more BM blasts and occurred more often after infusion of higher CAR–T cell doses. The severity of toxicity correlated with higher peak levels of $CD4^+$ and $CD8^+$ CAR–T cells in blood and higher peak IFN-γ and IL-6 concentrations in serum. Taken together, these data imply that a variable cell-dosing strategy may prove optimal for treating B-ALL with CAR–T cells. Patients with higher tumor burden may be best treated initially with a low CAR–T cell dose to minimize toxicity, whereas those with lower tumor burden may require higher or repeated doses of CAR–T cells to ensure recognition of a minimal tumor antigen load.

The frequency and clinical spectrum of toxicities occurring during CD19 CAR–T cell dose escalation were similar to those in other published studies in B-ALL, suggesting that therapy with an appropriate dose of a potent defined composition product per se does not increase the risk of toxicity. "Classical" CRS with fever, capillary leak, and hypotension requiring intensive care was frequent, but responded rapidly to tocilizumab (4–8 mg/kg i.v.) and dexamethasone (10 mg bid i.v.), with defervescence occurring within hours and discharge from the ICU within 1 to 2 days in most patients. Neurotoxicity was manifest by signs that included encephalopathy and seizures and focal deficits; in some patients, it followed a time course that was distinct from that of CRS. Neurologic signs often reached maximal severity after resolution of CRS and were not clearly responsive to intervention with tocilizumab or corticosteroids at either low or high doses.

We investigated whether surrogate markers of systemic inflammation could identify patients with sCRS and potentially be used to guide intervention to either suppress cytokine release or eliminate CAR–T cells in the event of severe toxicity. Serum ferritin and CRP concentrations correlated with the severity of acute toxicity and declined in response to tocilizumab or corticosteroids; however, additional data are needed to determine their utility in monitoring the response to CRS therapy. Severe hyperferritinemia (> 20,000 ng/ml) is not typically observed in infections even in heavily transfused patients (24) and could serve as a useful tool in distinguishing sCRS from other causes of fever after CAR–T cell infusion. Serum concentrations of IL-6 and IFN-γ also correlated with the severity of toxicity and had predictive value, with high concentrations within 1 day after CAR–T cell infusion identifying patients who subsequently developed severe neurotoxicity. If these findings are confirmed in additional patients, analysis of serum IL-6 and IFN-γ concentrations early after CAR–T cell infusion might be employed to identify patients at risk of life-threatening toxicity in whom early and aggressive intervention to mitigate immune cell cytokine production might be evaluated.

Although CAR–T cells induced CR in a majority of patients in our study, disease relapse occurred in a subset of patients. Leukemia relapse after CAR–T cells could be classified into 2 distinct phenotypes: those with loss of the CD19 target antigen as observed by others (25) and those that remained $CD19^+$ and relapsed in a manner associated with loss of CD19 CAR–T cells in blood. Two patients in our study relapsed with $CD19^-$ disease, 1 with B-ALL and 1 with a myeloid phenotype switch. $CD19^+$ relapse occurred exclusively in patients who did not have persisting CAR–T cells in blood; retreatment of these patients with a second CAR–T cell infusion did not result in CAR–T cell proliferation, persistence, or antitumor activity. We demonstrated that the loss of CAR–T cells was due to development of $CD8^+$ T cell immunity to the CAR transgene product. Because all CD19 CARs used in reported clinical trials of CD19 CAR–T cell therapy incorporate a murine scFv, these data provide one potential mechanism for the loss of CAR–T cells observed in other trials (2–8, 23, 26). A solution that may reduce immunogenicity of the construct would be to incorporate a human rather than murine CD19-specific scFv into the CAR construct.

Our trial investigated whether the addition of Flu to the lymphodepletion regimen could delay or abrogate development of anti-CAR immune responses and improve CAR–T cell expansion and persistence. We noted remarkably higher $CD4^+$ and $CD8^+$ CAR–T cell proliferation and persistence in patients who received Flu compared with those who did not receive Flu. The mechanisms by which Flu increased CAR–T cell accumulation and persistence could include greater lymphodepletion, resulting in increased levels of homeostatic cytokines that support T cell proliferation and survival, delaying or preventing the anti-CAR immune responses and potentially modifying the tumor microenvironment to

improve accessibility and stimulation of CAR–T cells. Consistent with the increased CAR–T cell expansion and persistence in patients who received Flu, we noted an improvement in DFS, albeit with a relatively short duration of follow-up. Only 1 of 17 patients (6%) who received Flu-containing lymphodepletion followed by CAR–T cells of defined composition developed CD19$^+$ relapse, and this occurred in a patient who, subsequent to achieving remission after CAR–T cell therapy, had an allogeneic HCT that resulted in elimination of the CAR–T cells. While these data are encouraging, additional patient accrual and longer follow-up are required.

We believe this study is the largest reported series of adult B-ALL patients treated with CD19 CAR–T cells and the first to demonstrate the feasibility of selecting defined T cell subsets for CAR engineering and formulation of defined therapeutic products for adoptive therapy. Data from this phase I/II trial demonstrate potent antitumor activity and reveal dose/response and dose/toxicity relationships that have not been clearly evident in CAR–T cell trials using unselected cells. The development of novel clinical cell isolation technologies that utilize flow cytometry cell sorting or serial column-based selections after labeling with reversibly binding reagents may further refine the selection of T cells with a complex immunophenotype and facilitate manufacturing defined CAR–T cell products for clinical evaluation (18, 27, 28).

Methods

Study design and patient selection. We performed a phase I/II open-label trial to evaluate the feasibility of manufacturing CD19 CAR–T cells formulated in a defined ratio of CD8$^+$ and CD4$^+$ T cell subsets and to assess the safety and efficacy of this therapy in patients with relapsed or refractory CD19$^+$ B cell malignancies. This manuscript reports the data from B-ALL patients in the study. There were no exclusion criteria for leukapheresis, CD19 CAR–T cell manufacturing, lymphodepletion chemotherapy, or CD19 CAR–T cell infusion based on the absolute lymphocyte count, the results of a test in vitro stimulation, or the presence or number of leukemia blasts in the peripheral blood. The study has been registered at ClinicalTrials.gov (NCT01865617).

T cell subset selection and CD19 CAR–T cell manufacturing. Peripheral blood mononuclear cells (PBMCs) were collected by leukapheresis, and the product was divided into 2 aliquots for enrichment of CD4$^+$ and CD8$^+$ T cell subsets for CAR–T cell manufacturing (Supplemental Figure 1). CD4$^+$ T cells were selected from 1 aliquot by positive immunomagnetic selection using the CliniMACS CD4 Reagent System (Miltenyi Biotec). CD8$^+$ T_{CM} cells were enriched from the second aliquot using a 2-step CliniMACS selection procedure involving depletion of CD4$^+$, CD14$^+$, and CD45RA$^+$ cells, followed by selection of CD62L$^+$ cells from the CD4$^-$CD14$^-$CD45RA$^-$ fraction as described (18). In patients with an absolute CD8$^+$ T_{CM} cell count of less than 20/μl, either the CD62L$^+$ selection was omitted or bulk CD8$^+$ T cells were selected using the CliniMACS CD8 Reagent System.

We designed a CAR comprising an FMC63-derived CD19-specific scFv fused to a modified IgG4-hinge spacer, a CD28 transmembrane domain, a 4-1BB costimulatory domain, and a CD3ζ signaling domain (29). To enable precise measurement of transduced CD4$^+$ and CD8$^+$ CAR–T cells, we incorporated EGFRt separated from the CD19 CAR by a T2A ribosomal skip sequence, which allowed identification of transduced T cells using flow cytometry after staining with the anti-EGFR monoclonal antibody, cetuximab (29, 30). The enriched CD4$^+$ and CD8$^+$ T cell subsets were separately stimulated with Dynabeads CD3CD28 CTS paramagnetic beads, transduced with the lentivirus encoding the CD19-specific CAR and EGFRt, and then cultured in 50 U/ml IL-2. After removal of CD3CD28 beads, the CD4$^+$ and CD8$^+$ T cells were separately stimulated with an irradiated CD19$^+$ EBV LCL and cultured in media supplemented with 50 U/ml IL-2. CAR–T cell manufacturing was completed within 15 to 20 days after initial bead stimulation. Quality assessments were performed separately on the cultured CD4$^+$ and CD8$^+$ CAR–T cells, and the 2 fractions were formulated in a 1:1 ratio of CD3$^+$CD4$^+$EGFRt$^+$:CD3$^+$CD8$^+$EGFRt$^+$ cells for infusion.

Lymphodepletion chemotherapy. To deplete endogenous lymphocytes prior to adoptive transfer of CAR–T cells, patients received 1 of 4 chemotherapy regimens: 2–4 g/m^2 Cy i.v. on day 1 (n = 11); 2–3 g/m^2 Cy i.v. on day 1 and 100 mg/m^2/d etoposide i.v. on days 1 to 3 (n = 2); and 60 mg/kg Cy i.v. on day 1 and 25 mg/m^2/d Flu i.v. on either days 2 to 4 or days 2 to 6 for patients who had previously received an allogeneic HCT and/or were considered at increased risk of toxicity (n = 17; Table 1).

CAR–T cell infusion. CD19 CAR–T cells were administered i.v. to each patient at or as close as possible to 1 of 3 cell DLs (DL1, 2×10^5 EGFRt$^+$ cells/kg, n = 13; DL2, 2×10^6 EGFRt$^+$ cells/kg, n = 15; DL3, 2×10^7 EGFRt$^+$ cells/kg, n = 2) 48 to 96 hours after completing chemotherapy. CD4$^+$ and CD8$^+$ CAR–T cells were successfully manufactured for all patients; however, CAR–T cells from 3 patients were not formulated at the defined 1:1 ratio of CD4$^+$:CD8$^+$ T cells due to insufficient growth of CD4$^+$ or CD8$^+$ CAR–T cells in culture (DL2, n = 2; DL3, n = 1). Two patients received cryopreserved CAR–T cells, whereas the remainder were formulated and infused without cryopreservation.

Clinical response assessment. BM aspirates and biopsies were obtained from each patient before lymphodepletion chemotherapy and approximately 2 to 4 weeks after CAR–T cell infusion. CR was defined as absence of immunophenotypically abnormal blasts in the BM by morphology and flow cytometry (limit of detection 1:10,000) and, in those patients with a known molecular marker of their leukemia, the absence of abnormalities by conventional karyotyping, FISH, or QPCR. When available, an aliquot of each BM aspirate was submitted for IGH deep sequencing (Adaptive Biotechnologies) from patients who attained CR. Patients with CNS leukemia identified before lymphodepletion chemotherapy underwent CSF sampling for flow cytometry analysis after CAR–T cell therapy. Patients with extramedullary disease underwent whole-body PET-CT imaging before and after CAR–T cell therapy. Toxicity was graded using the NCI CTCAE (v4.03).

Assessment of CAR–T cell persistence. Blood samples were obtained from patients before and at intervals after CAR–T cell infusion, and flow cytometry was performed to identify CD4$^+$ and CD8$^+$ CAR–T cells as viable CD45$^+$CD3$^+$CD4$^+$CD8$^-$EGFRt$^+$ or CD45$^+$CD3$^+$CD4$^-$CD8$^+$EGFRt$^+$ events, respectively. Absolute CAR–T cell counts were determined by multiplying the percentage of CAR–T cells identified by flow cytometry in a CD45$^+$ forward scatter–side scatter (FS-SS) lymphocyte gate by the absolute lymphocyte count established by a complete blood count (CBC) performed on the same day. To establish loss of CAR–T cell persistence due to an anti-CAR transgene immune response, we used QPCR to detect integrated transgene sequence.

Evaluation of serum cytokines. Serum concentrations of IFN-γ, IL-6, and TNF-α were evaluated by Luminex assay, according to the manufacturer's instructions.

Evaluation of transgene immunogenicity. We evaluated CD8+ T cell immune responses to the CAR transgene using a modification of an assay we previously developed in our lab (19). Cryopreserved PBMCs collected from patients before lymphodepletion chemotherapy and approximately 4 weeks after CAR–T cell infusion were stimulated twice at 7-day intervals with autologous irradiated CAR–T cells and IL-2. The preinfusion and postinfusion PBMC cultures were assayed for lysis of autologous CAR–T cells and autologous nontransduced T cells in a ^{51}chromium release assay. An immune response against the CAR transgene was defined as the presence of specific lysis of autologous CAR–T cells by postinfusion PBMC cultures, but not of autologous nontransduced T cells or autologous CAR–T cell by preinfusion PBMC cultures.

Statistics. Comparisons of continuous variables between groups were made using the Wilcoxon rank-sum test. The correlation between 2 continuous variables was assessed using linear regression, with the values of some variables replaced by their ranks due to relatively large values for some of the parameters (ferritin, CRP, IFN-γ, IL-6). Univariate and stepwise multivariate logistic regression were performed to assess predictors for the occurrence of severe neurotoxicity. No adjustments were made for multiple comparisons. The absolute CD4+ and CD8+ EGFRt+ CAR–T cell counts and their percentages within the parental subset were compared using the Mann-Whitney *U* test. DFS was determined as the time from CAR–T cell infusion until failure, defined as death or the detection of relapsed or persistent disease by morphologic, flow cytometry, karyotyping, FISH, and/or QPCR studies. We compared the group who received Cy/Flu lymphodepletion and the group who received Cy-based lymphodepletion without Flu using the log-rank test, where $P = 0.001$. Significant was defined as $P < 0.05$.

Study approval. This study was conducted according to the principles of the Declaration of Helsinki and with the approval of the FHCRC Institutional Review Board. Written, informed consent was obtained from all patients after a discussion of the possible risks and adverse effects of the therapy.

Author contributions

CJT, SRR, and DGM designed the trial and experiments and wrote the paper. LAH, CB, KM, BP, TMB, ER, and NS performed experiments. LAH, MH, DS, SC, LS, XC, CY, BW, SH, JC, and MCJ designed experiments. CC collected research data. TAG and DL analyzed statistical data.

Acknowledgments

The authors would like to thank the FHCRC Cell Processing Facility and Seattle Cancer Care Alliance (SCCA) Cell Therapy Laboratory for assistance in CAR–T cell manufacturing; Kari Blankenship, Anna-Marie Kane, Franziska Sommermeyer, Sheila Gelder, Jennifer Lindquist, and the staff of the SCCA Immunotherapy Clinic for assistance with clinical care and data management; and the FHCRC Immune Monitoring Lab. C.J. Turtle is a Damon Runyon Clinical Investigator. Funding was provided by the following: NCI R01 CA136551; Life Science Development Fund; Juno Therapeutics; Bezos Family Immunotherapy Initiative.

Address correspondence to: Cameron J. Turtle, Clinical Research Division, Fred Hutchinson Cancer Research Center, 1100 Fairview Ave N, Seattle, Washington 98109, USA. Phone: 206.667.7073; E-mail: cturtle@fhcrc.org.

Michael Hudecek's present address is: Department of Medicine II, University of Wuerzburg, Wuerzburg, Germany.

1. Brentjens RJ, et al. Safety and persistence of adoptively transferred autologous CD19-targeted T cells in patients with relapsed or chemotherapy refractory B-cell leukemias. *Blood*. 2011;118(18):4817–4828.
2. Lee DW, et al. T cells expressing CD19 chimeric antigen receptors for acute lymphoblastic leukaemia in children and young adults: a phase 1 dose-escalation trial. *Lancet*. 2015;385(9967):517–528.
3. Maude SL, et al. Chimeric antigen receptor T cells for sustained remissions in leukemia. *N Engl J Med*. 2014;371(16):1507–1517.
4. Davila ML, et al. Efficacy and toxicity management of 19-28z CAR T cell therapy in B cell acute lymphoblastic leukemia. *Sci Transl Med*. 2014;6(224):224ra25.
5. Kochenderfer JN, et al. B-cell depletion and remissions of malignancy along with cytokine-associated toxicity in a clinical trial of anti-CD19 chimeric-antigen-receptor-transduced T cells. *Blood*. 2012;119(12):2709–2720.
6. Kochenderfer JN, et al. Donor-derived CD19-targeted T cells cause regression of malignancy persisting after allogeneic hematopoietic stem cell transplantation. *Blood*. 2013;122(25):4129–4139.
7. Kochenderfer JN, et al. Chemotherapy-refractory diffuse large B-cell lymphoma and indolent B-cell malignancies can be effectively treated with autologous T cells expressing an anti-CD19 chimeric antigen receptor. *J Clin Oncol*. 2015;33(6):540–549.
8. Porter DL, Levine BL, Kalos M, Bagg A, June CH. Chimeric antigen receptor-modified T cells in chronic lymphoid leukemia. *N Engl J Med*. 2011;365(8):725–733.
9. Porter DL, et al. Chimeric antigen receptor T cells persist and induce sustained remissions in relapsed refractory chronic lymphocytic leukemia. *Sci Transl Med*. 2015;7(303):303ra139.
10. Lee DW, et al. Current concepts in the diagnosis and management of cytokine release syndrome. *Blood*. 2014;124(2):188–195.
11. Riddell SR, et al. Adoptive therapy with chimeric antigen receptor-modified T cells of defined subset composition. *Cancer J*. 2014;20(2):141–144.
12. Berger C, Jensen MC, Lansdorp PM, Gough M, Elliott C, Riddell SR. Adoptive transfer of effector CD8+ T cells derived from central memory cells establishes persistent T cell memory in primates. *J Clin Invest*. 2008;118(1):294–305.
13. Gattinoni L, et al. A human memory T cell subset with stem cell-like properties. *Nat Med*. 2011;17(10):1290–1297.
14. Stemberger C, Neuenhahn M, Gebhardt FE, Schiemann M, Buchholz VR, Busch DH. Stem cell-like plasticity of naïve and distinct memory CD8+ T cell subsets. *Semin Immunol*. 2009;21(2):62–68.
15. Turtle CJ, et al. Innate signals overcome acquired TCR signaling pathway regulation and govern the fate of human CD161hi CD8α+ semi-invariant T cells. *Blood*. 2011;118(10):2752–2762.
16. Wang X, Berger C, Wong CW, Forman SJ, Riddell SR, Jensen MC. Engraftment of human central memory-derived effector CD8+ T cells in immunodeficient mice. *Blood*. 2011;117(6):1888–1898.
17. Sommermeyer D, et al. Chimeric antigen receptor-modified T cells derived from defined CD8+ and CD4+ subsets confer superior antitumor reactivity in vivo. *Leukemia*. 2016;30(2):492–500.
18. Terakura S, Yamamoto TN, Gardner RA, Turtle CJ, Jensen MC, Riddell SR. Generation of CD19-chimeric antigen receptor modified CD8+ T cells derived from virus-specific central memory T cells. *Blood*. 2012;119(1):72–82.
19. Berger C, Flowers ME, Warren EH, Riddell SR. Analysis of transgene-specific immune responses that limit the in vivo persistence of adoptively transferred HSV-TK-modified donor T cells after allogeneic hematopoietic cell transplantation. *Blood*. 2006;107(6):2294–2302.
20. Riddell SR, et al. T-cell mediated rejection of gene-modified HIV-specific cytotoxic T lymphocytes in HIV-infected patients. *Nat Med*. 1996;2(2):216–223.
21. Singh N, Perazzelli J, Grupp SA, Barrett DM. Early memory phenotypes drive T cell proliferation in patients with pediatric malignancies. *Sci Transl Med*. 2016;8(320):320ra3.
22. Graef P, et al. Serial transfer of single-cell-

derived immunocompetence reveals stemness of CD8+ central memory T cells. *Immunity*. 2014;41(1):116–126.
23. Brentjens RJ, et al. CD19-targeted T cells rapidly induce molecular remissions in adults with chemotherapy-refractory acute lymphoblastic leukemia. *Sci Transl Med*. 2013;5(177):177ra38.
24. Wormsbecker AJ, Sweet DD, Mann SL, Wang SY, Pudek MR, Chen LY. Conditions associated with extreme hyperferritinaemia (>3000 μg/L) in adults. *Intern Med J*. 2015;45(8):828–833.
25. Sotillo E, et al. Convergence of acquired mutations and alternative splicing of CD19 enables resistance to CART-19 immunotherapy. *Cancer Discov*. 2015;5(12):1282–1295.
26. Kalos M, et al. T cells with chimeric antigen receptors have potent antitumor effects and can establish memory in patients with advanced leukemia. *Sci Transl Med*. 2011;3(95):95ra73.
27. Odendahl M, et al. Clinical-scale isolation of 'minimally manipulated' cytomegalovirus-specific donor lymphocytes for the treatment of refractory cytomegalovirus disease. *Cytotherapy*. 2014;16(9):1245–1256.
28. Pollack SM, et al. Tetramer guided, cell sorter assisted production of clinical grade autologous NY-ESO-1 specific CD8+ T cells. *J Immunother Cancer*. 2014;2(1):36.
29. Hudecek M, et al. The nonsignaling extracellular spacer domain of chimeric antigen receptors is decisive for in vivo antitumor activity. *Cancer Immunol Res*. 2015;3(2):125–135.
30. Wang X, et al. A transgene-encoded cell surface polypeptide for selection, in vivo tracking, and ablation of engineered cells. *Blood*. 2011;118(5):1255–1263.